Inorganic Chemistry

Article

pubs.acs.org/IC

Slow Magnetic Relaxation in Two New 1D/0D Dy^{III} Complexes with a Sterically Hindered Carboxylate Ligand

Sui-Jun Liu,[†] Jiong-Peng Zhao,[†] Wei-Chao Song,[†] Song-De Han,[†] Zhong-Yi Liu,[‡] and Xian-He Bu*[,†]

[†]Department of Chemistry and TKL of Metal- and Molecule-Based Material Chemistry, Nankai University, Tianjin 300071, China

[‡]College of Chemistry and TKL of Structure and Performance for Functional Molecules, Tianjin Normal University, Tianjin 300387, China

Supporting Information

ABSTRACT: Two carboxylate-bridged Dy^{III} complexes, $[Dy_2(piv)_5(\mu_3\text{-}OH)(H_2O)]_n$ (**1**) and $[Dy_2(piv)_6(phen)_2]$ (**2**) (pivH = pivalic acid; phen = 1,10-phenanthroline), have been synthesized and structurally characterized. Complex **1** takes a one-dimensional (1D) chain structure based on $[Dy_4(\mu_3\text{-}OH)_2(piv)_8(H_2O)_2]^{2+}$ units, while complex **2** is a dinuclear structure bridged by *syn,syn*-carboxylates. Magnetic investigation indicates weak ferromagnetic interaction between adjacent Dy^{III} ions of the Dy_4 unit in **1** and weak intramolecular antiferromagnetic interaction between Dy^{III} ions and/or depopulation of the Dy^{III} excited-state Stark sublevels in **2**. Alternating-current susceptibility measurements revealed frequency- and temperature-dependent out-of-phase signals under a zero direct-current field in **1**, with typical slow magnetic relaxation behavior with an anisotropic barrier $U \approx 4.5$ K, while **2** exhibits field-induced single-molecule-magnet behavior with $\Delta E/k_B = 28.43$ K under a 2 kOe external field.

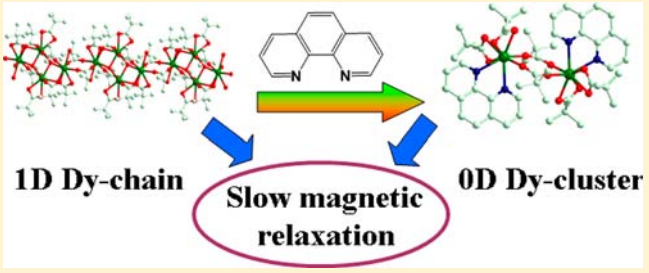

INTRODUCTION

Considerable interest has been focused on the study of single-molecule magnets (SMMs) since the 1990s because of their potential applications in information storage and quantum computing at the molecular level.[1] It is well-known that SMMs have unique properties such as slow magnetic relaxation and magnetic hysteresis.[2] To date, Co^{II}, Mn^{III}, Fe^{III}, and some other ions in the first-row transition metals (TMs) are good candidates in synthesizing SMMs,[3] because of the relatively large spin ground state (S) and/or magnetoanisotropy (D), which will eventually result in an anisotropic energy barrier (U_{eff}) that prevents reversal of the molecular magnetization.[4] A large number of cluster-based SMMs have been reported, but most of such studies were focused on TM SMMs.[5] Lanthanide (Ln) complexes [especially for dysprosium (Dy) chains and clusters] have recently become favorable candidates for exploring the kinds of magnetic phenomena in the field of molecular magnets, especially in their SMM types, because of their significant magnetic anisotropy and large energy barriers.[4a,6] In addition, SMMs based on Dy clusters or chains are limited because of the different affinities and capabilities of the Dy^{III} ions to O and N donors.[7] Thus, the design and construction of Dy^{III} SMMs still remains a great challenge and attracts great attention.

As is known, many factors such as solvents, counteranions, pH value, temperature, and molar ratio between reactants can influence the formation of Dy^{III} complexes.[8] However, one important consideration in the design of target complexes is the selection of appropriate ligands with bridging and/or terminal groups that can efficiently coordinate to metal ions.[9] Carboxylate-based ligands have been widely used to construct 3d metal complexes with various structures and interesting magnetic properties; nonetheless, they are rarely used for building Ln-based SMMs, probably because of the very weak coupling between Ln ions bridged by carboxylates.[10] Additionally, magnetic interaction for the Dy^{III} system including a carboxylate ligand is complicated and difficult to explain because many factors, especially the strong spin−orbit coupling, can lead to the $4f^n$ configuration splitting into $^{2S+1}L_J$ states and finally into Stark components under the ligand-field (LF) perturbation.[3a,11] To design and assemble ferromagnetic/ferrimagnetic cluster or chain complexes with carboxylate ligands, a hydroxyl group or other short bridging groups should be introduced to strengthen the coupling interaction.[12] As an important chelate-bridging and sterically hindered carboxylate ligand, pivalic acid (pivH) has been well employed to synthesize low-dimensional structures, such as Dy_4,[12a] Cr_4Dy_4,[13a] Ni_6Gd_6,[13b] and Fe_7Dy_4.[13c]

Employing pivH as the primary ligand and introducing Dy_2O_3 as the ion source, we may facilitate the formation of low-dimensional Dy^{III} complexes. Notably, a hydroxyl group can be generated in situ because Dy_2O_3 in the acidic system may promote water to form hydroxide. Moreover, as an effective terminal coligand, 1,10-phenanthroline (phen) may reduce the dimensionality of polymeric complexes. Arising from the

Received: November 15, 2012
Published: February 4, 2013

   dx.doi.org/10.1021/ic302496g | *Inorg. Chem.* 2013, 52, 2103−2109

ferromagnetic interaction and/or strong magnetic anisotropy of Dy^{III} ions, Dy chains and clusters with slow magnetic relaxation could be expected to be obtained (see Scheme 1). As an extension of our studies on the synthesis and magnetic properties of 3d-only and Ln-3d-block low-dimensional magnets,[14] we report herein two new Dy^{III} complexes, $[Dy_2(piv)_5(\mu_3\text{-}OH)(H_2O)]_n$ (**1**) with one-dimensional (1D) chain structure and $[Dy_2(piv)_6(phen)_2]$ (**2**) with dinuclear structure. Magnetic analyses reveal that **1** and **2** are both weakly coupled, displaying slow relaxation of the magnetization behavior. To the best of our knowledge, a 1D chain Dy^{III} complex with slow magnetic relaxation, synthesized from a pure carboxylate ligand and metal oxide, has not been reported yet.

Scheme 1. Scheme for the Design of Complexes 1 and 2

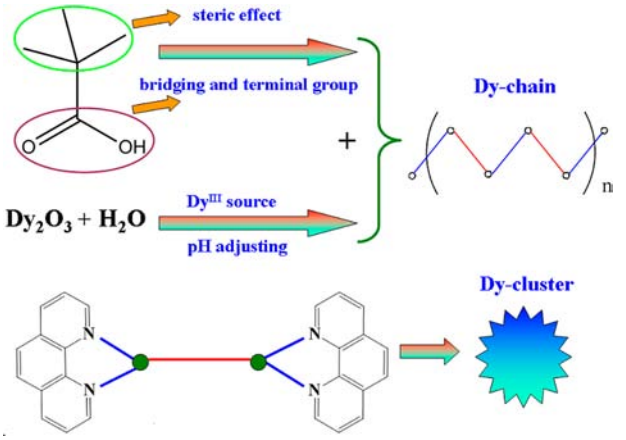

EXPERIMENTAL SECTION

Materials and General Methods. All of the starting materials for synthesis were commercially available and were used as received. Elemental analyses of C, H, and N were carried out with a Perkin-Elmer 240C analyzer. IR spectra were measured on a TENSOR 27 (Bruker) FT-IR spectrometer with KBr pellets in the range 4000−400 cm^{-1}. The powder X-ray diffraction (PXRD) spectra were recorded on a Rigaku D/Max-2500 diffractometer at 40 kV and 100 mA for a Cu-target tube and a graphite monochromator. Simulation of the PXRD spectra was carried out by the single-crystal data and diffraction-crystal module of the *Mercury* program available free of charge. Magnetic data were collected using crystals of the samples on a Quantum Design MPMS-XL-7 SQUID magnetometer equipped. The data were corrected using Pascal's constants to calculate the diamagnetic susceptibility, and an experimental correction for the sample holder was applied.

Synthesis of Complexes 1 and 2. *$[Dy_2(piv)_5(\mu_3\text{-}OH)(H_2O)]_n$ (**1**).* A mixture of Dy_2O_3 (0.5 mmol, 0.186 g), pivH (2 mmol, 0.204 g), and H_2O (10 mL) was sealed in a 23 mL Teflon-lined autoclave and heated to 160 °C. After being maintained for 72 h, the reaction vessel was cooled to room temperature in 12 h. Colorless crystals were collected with ca. 20% yield based on pivH. Anal. Calcd for $C_{25}H_{48}Dy_2O_{12}$: C, 34.69; H, 5.59. Found: C, 35.08; H, 5.18. FT-IR (KBr pellets, cm^{-1}): 3384s, 2965s, 2926m, 2869m, 1542s, 1489s, 1432s, 1361s, 1228s, 1029w, 902m, 850w, 810m, 792m, 614m, 561m.

*$[Dy_2(piv)_6(phen)_2]$ (**2**).* A mixture of Dy_2O_3 (0.5 mmol, 0.186 g), pivH (2 mmol, 0.204 g), 1,10-phenanthroline monohydrate (0.5 mmol, 0.0991 g), and H_2O (10 mL) was sealed in a 23 mL Teflon-lined autoclave and heated to 160 °C. After being maintained for 72 h, the reaction vessel was cooled to room temperature in 12 h. Colorless crystals were collected with ca. 10% yield based on pivH. Anal. Calcd for $C_{54}H_{70}Dy_2N_4O_{12}$: C, 50.19; H, 5.46; N, 4.34. Found: C, 49.97; H, 5.22; N, 4.36. FT-IR (KBr pellets, cm^{-1}): 3397m, 3073m, 2956s, 2922s, 2865s, 1592s, 1518s, 1485s, 1428s, 1361s, 1229s, 1137m, 1101m, 897m, 855w, 807m, 734m, 607m, 420m.

Crystallographic Data and Structure Refinements. The single-crystal X-ray diffraction data were collected on a Rigaku SCX-mini diffractometer at 293(2) K with Mo Kα radiation (λ = 0.71073 Å) by ω scan mode. The program *SAINT*[15] was used for integration of the diffraction profiles. The structures were solved by direct methods using the *SHELXS* program of the *SHELXTL* package and refined by full-matrix least-squares methods with *SHELXL* (semiempirical absorption corrections were applied using the *SADABS* program).[16] The non-H atoms were located in successive difference Fourier syntheses and refined with anisotropic thermal parameters on F^2. The H atoms of the ligands were generated theoretically at the specific atoms and refined isotropically with fixed thermal factors. The H atoms of water in **1** were not assigned, and the H atoms of the hydroxyl groups in **1** were added by the difference Fourier maps. A summary of the crystallographic data, data collection, and refinement parameters for **1** and **2** is provided in Table 1. The selected bond lengths and angles are given in Tables S1 and S2 (Supporting Information).

Table 1. Crystal Data and Structure Refinements for 1 and 2

	1	2
formula	$C_{25}H_{48}Dy_2O_{12}$	$C_{54}H_{70}Dy_2N_4O_{12}$
M_r	865.64	1292.14
cryst syst	monoclinic	triclinic
space group	$P2_1/n$	$P\bar{1}$
a [Å]	11.382(2)	10.321(2)
b [Å]	22.640(5)	11.966(2)
c [Å]	14.297(3)	12.772(3)
α [deg]	90	113.06(3)
β [deg]	106.49(3)	99.57(3)
γ [deg]	90	96.94(3)
V [Å^3]	3532.6(12)	1400.7(5)
ρ [g cm^{-3}]	1.624	1.532
Z	4	1
F(000)	1696	650
μ [mm^{-1}]	4.247	2.708
collected reflns	29740	12262
unique reflns	6225	4931
R(int)	0.1008	0.1001
R1[a]/wR2[b] [$I > 2\sigma(I)$]	0.0627/0.1046	0.0608/0.1544
GOF on F^2	1.098	1.114

[a] $R1 = \sum(||F_o| - |F_c||)/\sum|F_o|$. [b] $wR2 = [\sum w(|F_o|^2 - |F_c|^2)^2/(\sum w|F_o|^2)^2]^{1/2}$.

RESULTS AND DISCUSSION

Synthesis. In our efforts to obtain the target complexes, pivH with steric effects acts as both a bridging and a terminal ligand, and the introduction of phen is to obtain lower dimensional complexes. Generally, Ln^{III} complexes were mainly constructed by Ln^{III} salts as the source of the metal ion, and only a few examples using rare earth oxides under hydrothermal reactions were reported.[17] Herein, for the synthesis of **1** and **2**, Dy_2O_3 not only serves as a slow-release Dy^{III} ion source but also adjusts the pH value of the systems.

Structural Analysis. Complex **1** crystallizes in the monoclinic space group $P2_1/n$ with Z = 4. The asymmetric unit consists of two Dy^{III} ions (eight- and seven-coordinated, respectively), five piv ligands, one μ_3-OH^-, and one coordinated water molecule (range of the Dy−O length = 2.253(7)−2.587(7) Å; see Table S1 in the Supporting Information). Dy1 is surrounded by six carboxylate O atoms (O2B, O6, O7, O8A, O9, and O10) from five different piv

dx.doi.org/10.1021/ic302496g | Inorg. Chem. 2013, 52, 2103−2109

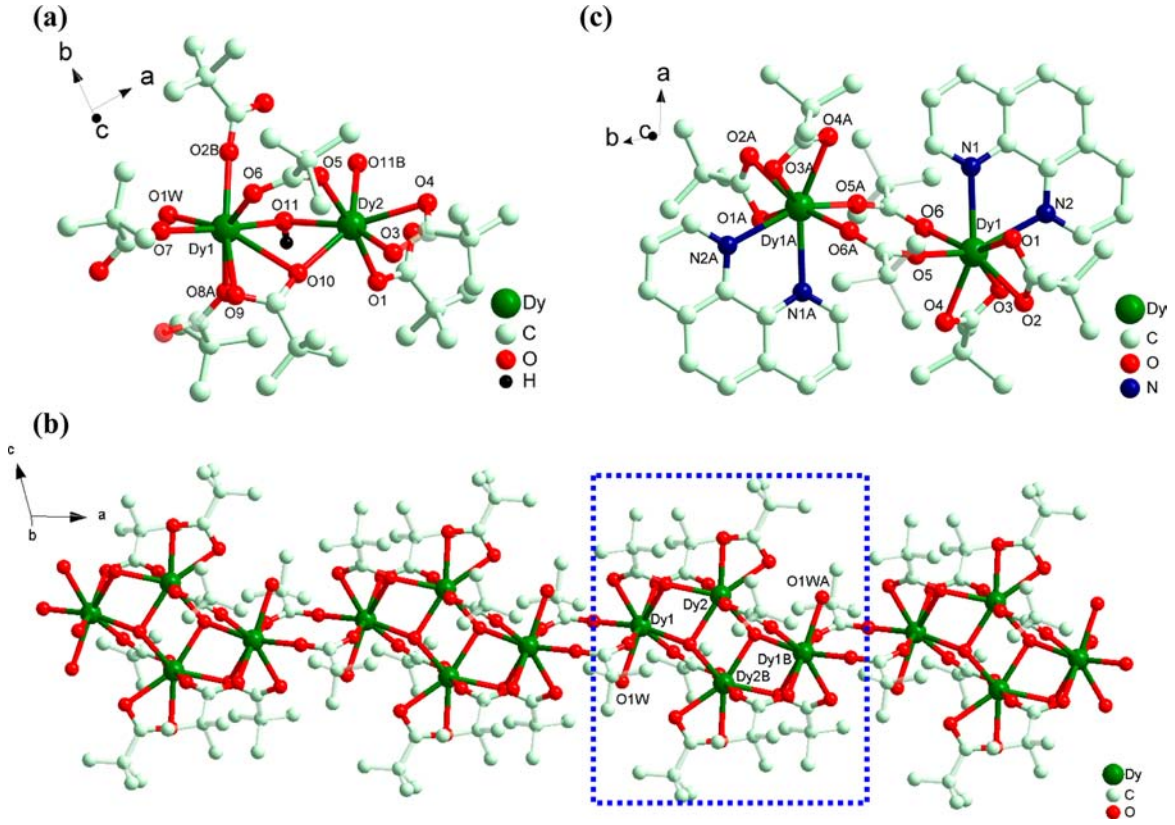

Figure 1. Views of (a) the coordination environment of Dy^{III} in **1** (H atoms of methyl and water omitted for clarity; symmetry codes: A, $-x + 1$, $-y + 2$, $-z$; B, $-x + 2$, $-y + 2$, $-z$), (b) the 1D chain structure of **1** (blue box for the $[Dy_4(\mu_3\text{-}OH)_2(piv)_8(H_2O)_2]^{2+}$ unit), and (c) the structure of **2** (H atoms omitted for clarity; symmetry code: A, $-x + 2$, $-y + 1$, $-z + 1$).

ligands, one O atom (O11) from OH^-, and one O atom (O1W) from a coordinated water molecule, while Dy2 is surrounded by six carboxylate O atoms (O1, O3, O4, O5, O10, and O11B) from five different piv ligands and one O atom (O11) of OH^- (Figure 1a). As shown in Figure 1b, Dy1 and Dy2 are bridged by carboxylate (μ_2-η^1:η^1 and μ_2-η^1:η^2 modes) and hydroxyl to generate a butterfly-shaped $[Dy_4(\mu_3\text{-}OH)_2(piv)_8(H_2O)_2]^{2+}$ unit with intratetramer $Dy^{3+}\cdots Dy^{3+}$ distances of 3.790–4.175 Å. The Dy–O–Dy angles range from 100.22° to 107.70°. The neighboring $[Dy_4(\mu_3\text{-}OH)_2(piv)_8(H_2O)_2]^{2+}$ units are further connected by two carboxylate groups with syn,syn mode to form a Dy-based 1D chain.

Complex **2** crystallizes in the triclinic space group $P\bar{1}$ with $Z = 1$. The molecular structure consists of one crystallographically independent Dy^{III} ion eight-coordinated by three piv ligands and one phen ligand. Dy1 is surrounded by six carboxylate O atoms (O1, O2, O3, O4, O5, and O6) from four different piv ligands and two N atoms (N1, N2) of a phen ligand. Unlike **1**, two piv and two phen ligands chelate one Dy^{III} ion. As shown in Figure 1c, Dy1 and Dy1A are bridged by two *syn,syn*-carboxylate groups with a $Dy^{3+}\cdots Dy^{3+}$ separation of 5.391 Å, which is significantly longer than that in **1**. Notably, the introduction of phen may be favorable to form low-dimensional structures.

Magnetic Properties. The magnetic properties of **1** and **2** were investigated by solid-state magnetic susceptibility measurements in the 2–300 K range at 1 kOe field and the isothermal field-dependent magnetizations $M(H)$ at fields up to 50 kOe (all of the measurements were carried out on crystalline samples and their phase purities confirmed by PXRD; see Figure S1 in the Supporting Information).

The magnetic properties of **1** and **2** in the form of $\chi_M T$ vs T plots are shown in Figure 2. At 300 K, the $\chi_M T$ values of **1** and **2** are 28.13 and 28.10 emu mol^{-1} K, respectively, consistent with the expected value of 28.34 emu mol^{-1} K for two uncoupled Dy^{III} ions ($^6H_{15/2}$, $L = 5$, and $g = {}^4/_3$).[18] For **1**, as the temperature decreases, the value of $\chi_M T$ slowly decreases down to a minimum value of 25.79 emu mol^{-1} K at 12 K. On cooling the temperature to 2 K, $\chi_M T$ abruptly increases to a maximum value (26.93 emu mol^{-1} K), indicating ferromagnetic coupling between Dy^{III} ions in the $[Dy_4(\mu_3\text{-}OH)_2(piv)_8(H_2O)_2]^{2+}$ unit. Notably, magnetic interaction of Dy^{III} ions between adjacent Dy_4 clusters is very weak and can be ignored. For **2**, the $\chi_M T$ value slowly decreases on cooling and then more rapidly below 140 K to a minimum value of 22.22 emu mol^{-1} K at 2 K, indicating weak intramolecular antiferromagnetic interactions and/or depopulation of the Dy^{III} excited-state Stark sublevels.[19] The Stark sublevels of the anisotropic Dy^{III} ions may be progressively thermally depopulated, leading to a decrease of the $\chi_M T$ value.[19]

The Curie–Weiss fitting $[\chi_M = C/(T - \theta)]$ of the magnetic data over the temperature ranges 20–300 and 2–300 K results in the Curie constant $C = 28.33$ emu mol^{-1} K and the Weiss constant $\theta = -2.65$ K for **1** and $C = 28.24$ emu mol^{-1} K and $\theta = -3.68$ K for **2**, respectively. For **1**, the negative θ value does not indicate dominant antiferromagnetic coupling between the Dy^{III} centers because strong spin–orbit coupling of the Dy^{III} ion can also lead to a negative θ value and a decrease of $\chi_M T$ at high temperature.[20] Thus, dominant weak ferromagnetic

dx.doi.org/10.1021/ic302496g | *Inorg. Chem.* 2013, 52, 2103–2109

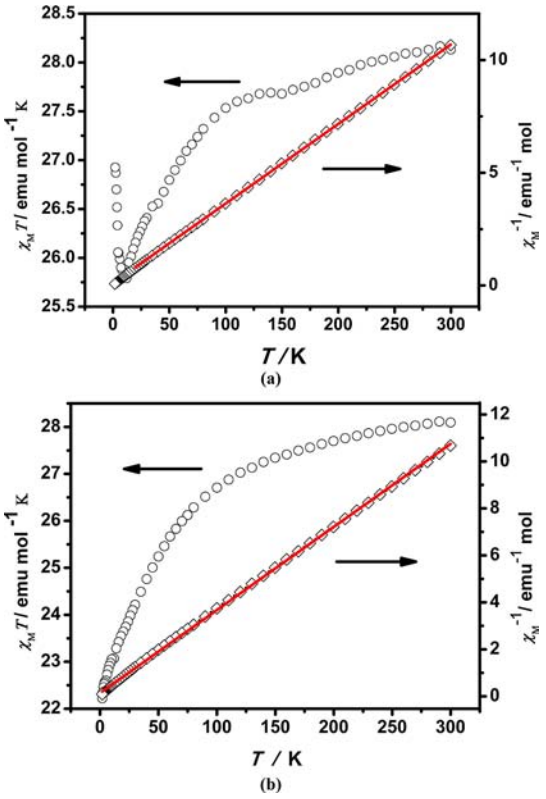

Figure 2. Temperature dependence of magnetic susceptibilities in the form of $\chi_M T$ (○) at an applied field of 1 kOe and χ_M^{-1} vs T plot (◇) (red part for the Curie–Weiss fitting) for **1** (a) and **2** (b).

interactions between adjacent Dy^{III} ions in the Dy_4 unit exist in **1**, which is in good agreement with the prediction that the Dy–Dy coupling is expected to be very weak because of shielding of the f orbitals and the consequent very small overlap with the bridging ligand orbitals.[21] For **2**, the small negative θ value is presumably caused by antiferromagnetic interaction and/or the crystal-field effect of the free Dy^{III} ion.

The M vs H curve (at 2 K) for **1** is shown in Figure 3. M increases quickly at very low field, reaching about 10.01 Nβ at

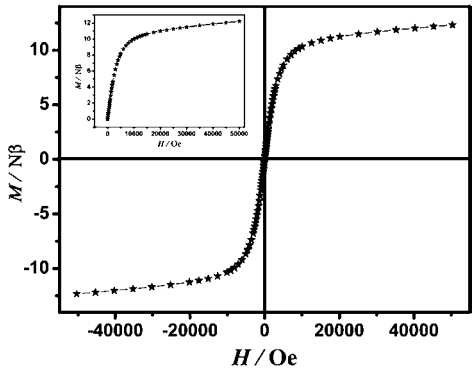

Figure 3. Field dependence of the magnetization of **1** measured at 2 K. Inset: M–H plot at 2 K.

10 kOe. In the high-field region, the increase of magnetization is slow and linear, which may be attributed to the anisotropy of the polycrystalline sample. The value of M reaches to 12.26 Nβ at 50 kOe, being far from the theoretical saturated value of 20 Nβ ($g_J \times J = {}^4/_3 \times {}^{15}/_2 = 10$ Nβ) anticipated for two independent Dy^{III} ions with $S = {}^5/_2$ ground state.[3a,22] It can be explained by the fact that depopulation of the Stark levels of the Ln^{III} $^{2S+1}L_J$ ground state under the LF perturbation produces a much smaller effective spin.[3a] In addition, the M vs H plot for **1** almost does not show hysteresis at 2 K because of the superlow blocking temperature, which is consistent with the subsequent alternating-current (ac) measurements in which no peak and only a tail of the out-of-phase signal down to 2 K appeared.

For **2**, the M vs H/T (Figure 4) data at 2.0–4.0 K show nonsuperposition plots and a rapid increase of the magnet-

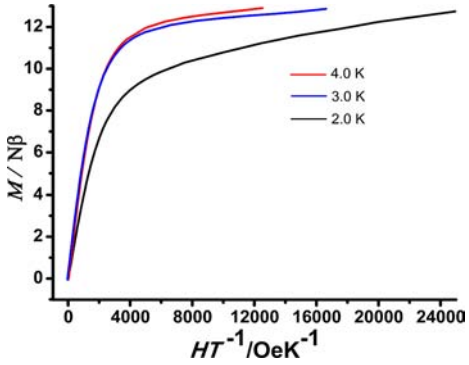

Figure 4. Plots of M vs H/T for **2** in the field range 0–50 kOe.

ization at low fields, which eventually reaches the value of 12.76 Nβ at 2.0 K and 50 kOe without any sign of saturation. The reason is most likely due to anisotropy and the important crystal-field effect at the Dy^{III} ion, which eliminates the 16-fold degeneracy of the $^6H_{15/2}$ ground state.[13a,23] Reduced magnetization curves do not superimpose, further indicating the presence of significant magnetic anisotropy and/or low-lying excited states.[13a,24]

Because of the very weak interaction between Dy_4 subunits, complex **1** may display SMM behavior. In order to further elucidate its possible SMM behavior, ac susceptibility measurements for **1** were performed in the temperature range 15–2 K under $H_{dc} = 0$ Oe and $H_{ac} = 3.5$ Oe for variable frequencies (from 997 to 3 Hz). A frequency-dependent out-of-phase signal appeared, yet all of the in-phase curves (χ') are almost consistent without peaks, indicating a slow relaxation behavior of the magnetization (Figure 5a). However, the maximum value of χ'' was not observed even up to 997 Hz because of the 2 K temperature limit of the instrument. The preexponential factor (τ_0) and energy barrier (U) to reverse the magnetization can be roughly estimated from the $\ln(\chi''_M/\chi'_M)$ vs $1/T$ plot at 997 Hz by considering a single relaxation time (Figure 5c). The least-squares fit of the experimental data through the expression $\chi''_M/\chi'_M = 2\pi\upsilon\tau_0 \exp(U/k_BT)$ gave $\tau_0 \approx 1.1 \times 10^{-7}$ s and $U \approx 4.5$ K for **1**.[25] In order to investigate the dynamic properties of the slow magnetic relaxation and obtain an effective energy barrier (U_{eff}) close to the theoretical one, strong fields of 2 and 5 kOe at 997 Hz were applied in ac measurements, and good peak shapes in phase (Supporting Information, Figure S2) but not out of phase (Supporting Information, Figure S3) were obtained. The peaks in phase appeared at 4 and 6.4 K, respectively. The ac signals suggested the existence of a quantum-tunneling effect at low temperature, which was not effectively suppressed. Because slow relaxation of the magnetization is experimentally observed only over a short range of temperature and no maximum of χ'' is found at technically available low temperatures, the estimation of these character-

dx.doi.org/10.1021/ic302496g | Inorg. Chem. 2013, 52, 2103–2109

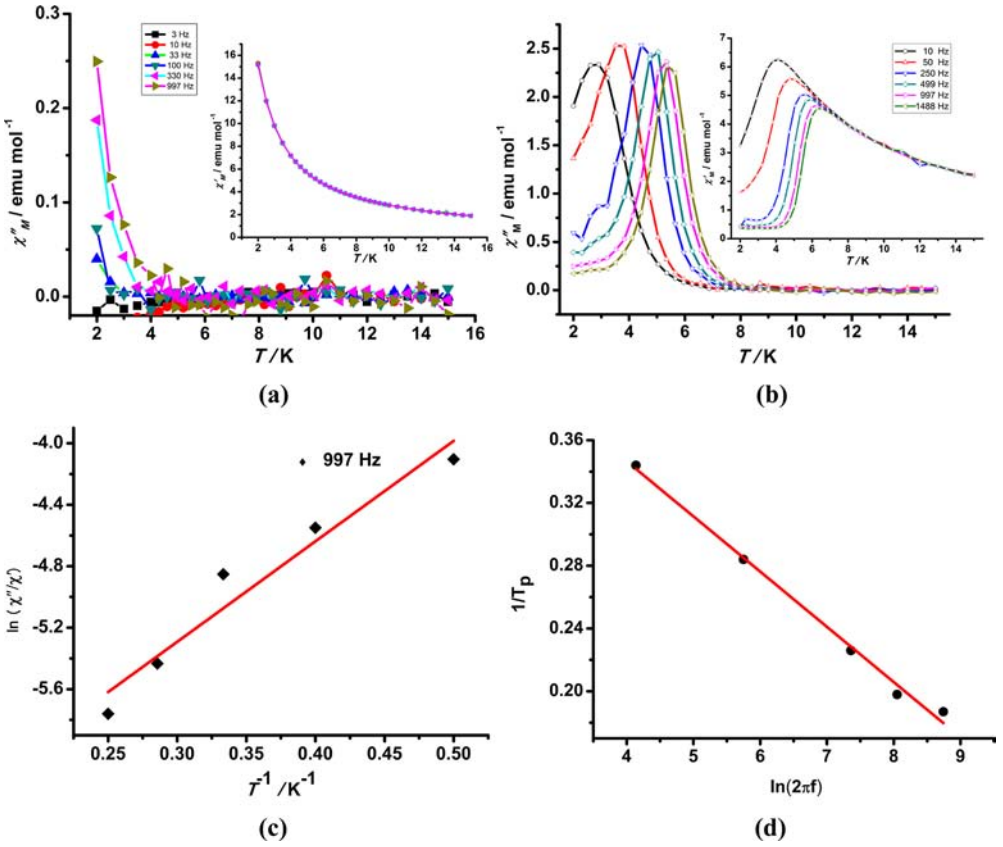

Figure 5. (a) Temperature dependence of the ac χ_M at different frequencies for **1** with H_{dc} = 0 Oe. (b) Temperature dependence of the ac χ_M at different frequencies for **2** with H_{dc} = 2 kOe. (c) $\ln(\chi''_M/\chi'_M)$ vs $1/T$ plot for **1** at 997 Hz of the 3.5 Oe ac field. The solid line is the best-fit curve. (d) Least-squares fit for **2** of the experimental data to the Arrhenius equation.

istic parameters might not be very accurate, but τ_0 agrees with the expected values ($\tau_0 = 10^{-6}$–10^{-11} s) for an SMM.[24,26] Thus, the observed behavior of **1** is consistent with SMM behavior.

To investigate the SMM behavior of complex **2**, ac susceptibility measurements for **2** were performed in the temperature range 15–2 K under H_{dc} = 0 Oe and H_{ac}= 3.5 Oe for variable frequencies (from 1488 to 10 Hz). As shown in Figure S4 (Supporting Information), all of the signals of χ' coincide without any peaks occurring; meanwhile, a weak frequency-dependent χ'' appears because of a strong quantum-tunneling effect. To weaken the quantum-tunneling effect, a suitable direct-current (dc) field needs to be exerted. The best field was found from field-dependent ac susceptibility measurements (0–5 kOe). As shown in Figure S5 (Supporting Information), the peak appeared at ca. 2 kOe. Thus, a 2 kOe dc field was exerted to reduce the strong quantum-tunneling effect. The peaks can be obviously observed in both the χ'_M and χ''_M curves (see Figure 5b), which suggests the existence of slow magnetic relaxation behavior in **2**.

To obtain the relaxation energy barrier and relaxation time of **2**, the peak temperature, T_p, can be given by the Lorentzian peak function fitted from the plots of χ''_M vs T, and the best fitting based on the Arrhenius law $1/T_p = -k_B/\Delta E[\ln(2\pi f) + \ln(\tau_0)]$ (f is the frequency) gave the energy barrier $\Delta E/k_B$ = 28.43 K and the preexponential factor $\tau_0 = 9.64 \times 10^{-7}$ s (Figure 5d). The values are in agreement with the observed preexponential factors and effective energy barriers for Dy^{III}-containing SMMs. Furthermore, at fixed temperatures of 2.0 and 3.0 K with a 300 Oe dc field, the Cole–Cole plots (Figure 6) from 0.1 to 1488 Hz in the form of χ''_M vs χ'_M can be fitted

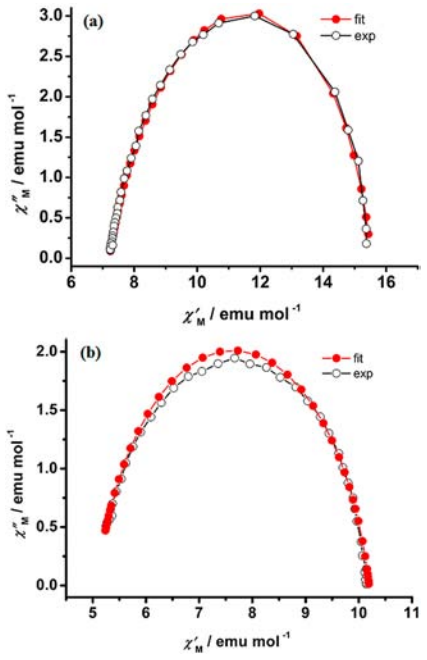

Figure 6. Cole–Cole plots for **2** measured at 2.0 K (a) and 3.0 K (b) with a 300 Oe dc field. The red lines are the best fit to the experimental data, obtained with the generalized Debye model.

by the generalized Debye functions to give α = 0.19, τ = 0.028, and α = 0.15, τ = 0.0016, respectively. The relatively small α values indicate the occurrence of a single relaxation process. To

dx.doi.org/10.1021/ic302496g | Inorg. Chem. 2013, 52, 2103–2109

further investigate the low-temperature relaxation behavior, variable-frequency ac susceptibility data were collected at 3.0 K under 2 and 3 kOe dc fields. At each dc field, multiple relaxation processes were observed (Supporting Information, Figure S6), which may be associated with distinct anisotropic centers in **2**.[19b,26,27] As aforementioned, strong anisotropy of Dy^{III} ions presumably result in the field-induced SMM behavior in **2**.

CONCLUSION

In this study, two new carboxylate-based Dy^{III} complexes with low-dimensional structures have been generated from a sterically hindered carboxylate ligand pivH, phen, and Dy_2O_3. The synthetic methods may allow for the assembly of other related chain- or cluster-based SMMs. Magnetic measurements indicate weak ferromagnetic interaction between Dy^{III} ions of the $[Dy_4(\mu_3\text{-}OH)_2(piv)_8(H_2O)_2]^{2+}$ unit in **1** and weak intramolecular antiferromagnetic interaction between Dy^{III} ions and/or depopulation of the Dy^{III} excited-state Stark sublevels in **2**. For **1**, no obvious χ'' peak but strong field-dependent χ' and χ'' signals were observed, suggesting slow magnetic relaxation and the existence of zero-field quantum tunneling at low temperature in this complex. For **2**, the properties of the single Dy^{III} ion may be directly responsible for the magnetic relaxation processes and SMM behavior because the intramolecular magnetic interaction between Dy^{III} ions is very weak in the dinuclear complex. Thus, the magnetic behavior of each Dy^{III} ion of **2** may have resulted in the appearance of good peak shape of the ac curves in a dc field. Therefore, this study provides a good example for the modulation of low-dimensional structures and their magnetic properties (from chain-based slow magnetic relaxation behavior to cluster-based SMM behavior).

ASSOCIATED CONTENT

Supporting Information

X-ray crystallographic data file in CIF format for CCDC 882180 (complex **1**) and 885140 (complex **2**), simulated and experimental PXRD (Figure S1) of **1** and **2**, magnetic data (Figures S2−S6) of **1** and **2**, and selected bond distances and angles for **1** and **2** (Tables S1 and S2). This material is available free of charge via the Internet at http://pubs.acs.org.

AUTHOR INFORMATION

Corresponding Author

*E-mail: buxh@nankai.edu.cn. Tel: +86-22-23502809. Fax: +86-22-23502458.

Notes

The authors declare no competing financial interest.

ACKNOWLEDGMENTS

This work was supported by the 973 Program of China (Grant 2012CB821700), the NSF of China (Grants 21031002 and 51073079), and the Natural Science Fund of Tianjin, China (Grant 10JCZDJC22100).

REFERENCES

(1) For examples, see: (a) Sessoli, R.; Gatteschi, D.; Caneschi, A.; Novak, M. A. *Nature* **1993**, *365*, 141. (b) Mills, D. P.; Moro, F.; McMaster, J.; Slageren, J. V.; Lewis, W.; Blake, A. J.; Liddle, S. T. *Nat. Chem.* **2011**, *3*, 454. (c) Schwöbel, J.; Fu, S. H.; Brede, J.; Dilullo, A.; Hoffmann, G.; Klyatsskaya, S.; Ruben, M.; Wiesendanger, R. *Nat. Commun.* **2012**, *3*, 953. (d) Gatteschi, D.; Sessoli, R. *Angew. Chem., Int. Ed.* **2003**, *115*, 278. (e) Liu, R. N.; Li, L. C.; Wang, X. L.; Yang, P. P.; Wang, C.; Liao, D. Z.; Sutter, J. P. *Chem. Commun.* **2010**, *46*, 2566. (f) Feng, X. W.; Liu, J. J.; Harris, T. D.; Hill, S.; Long, J. R. *J. Am. Chem. Soc.* **2012**, *134*, 7521. (g) Wang, H. L.; Wang, K.; Tao, J.; Jiang, J. Z. *Chem. Commun.* **2012**, *48*, 2973. (h) Leng, J. D.; Liu, J. L.; Zheng, Y. Z.; Ungur, L.; Chibotaru, L. F.; Guo, F. S.; Tong, M. L. *Chem. Commun.* **2013**, *49*, 158.

(2) (a) Bernot, K.; Bogani, L.; Caneschi, A.; Gatteschi, D.; Sessoli, R. *J. Am. Chem. Soc.* **2006**, *128*, 7947. (b) Wang, X. L.; Bao, X.; Xu, P. P.; Li, L. *Eur. J. Inorg. Chem.* **2011**, *50*, 3586. (c) Pointillart, F.; Gal, Y. L.; Golhen, S.; Cador, O.; Ouahab, L. *Chem.—Eur. J.* **2011**, *17*, 10397.

(3) (a) Wang, Y.; Li, X. L.; Wang, T. W.; Song, Y.; You, X. Z. *Inorg. Chem.* **2010**, *49*, 969. (b) Zheng, Y. Z.; Xue, W.; Tong, M. L.; Chen, X. M.; Zheng, S. L. *Inorg. Chem.* **2008**, *47*, 11202.

(4) (a) Langley, S. K.; Chilton, N. F.; Gass, I. A.; Moubaraki, B.; Murray, K. S. *Dalton Trans.* **2011**, *40*, 12656. (b) Papatriantafyllopoulou, C.; Wernsdorfer, W.; Abboud, K. A.; Christou, G. *Inorg. Chem.* **2011**, *50*, 421. (c) Rinehart, J. D.; Fang, M.; Evans, W. J.; Long, J. R. *Nat. Chem.* **2011**, *3*, 538.

(5) For examples, see: (a) Wang, Y. Q.; Sun, W. W.; Wang, Z. D.; Jia, Q. X.; Gao, E. Q.; Song, Y. *Chem. Commun.* **2011**, *47*, 6386. (b) Li, X. B.; Zhang, J. Y.; Wang, Y. Q.; Song, Y.; Gao, E. Q. *Chem.—Eur. J.* **2011**, *17*, 13883. (c) Ding, M.; Wang, B. W.; Wang, Z. M.; Zhang, J. L.; Fuhr, O.; Fenske, D.; Gao, S. *Chem.—Eur. J.* **2012**, *18*, 915. (d) Yoon, J. H.; Lee, J. W.; Ryu, D. W.; Yoon, S. W.; Suh, B. J.; Kim, H. C.; Hong, C. S. *Chem.—Eur. J.* **2011**, *17*, 3028. (e) Zhang, X. M.; Li, C. R.; Zhang, X. H.; Zhang, W. X.; Chen, X. M. *Chem. Mater.* **2008**, *20*, 2298.

(6) For examples, see: (a) Sulway, S. A.; Layfield, R. A.; Tuna, F.; Wernsdorfer, W.; Winpenny, R. E. P. *Chem. Commun.* **2012**, *48*, 1508. (b) Ren, J.; Liu, Y.; Chen, Z.; Xiong, G.; Zhao, B. *Sci. China Chem.* **2012**, *55*, 1073. (c) Tang, J. K.; Hewitt, I.; Madhu, N. T.; Chastanet, G.; Wernsdorfer, W.; Anson, C. E.; Benelli, C.; Sessoli, R.; Powell, A. K. *Angew. Chem., Int. Ed.* **2006**, *45*, 1729. (d) Guo, P. H.; Liu, J. L.; Zhang, Z. M.; Ungur, L.; Chibotaru, L. F.; Leng, J. D.; Guo, F. S.; Tong, M. L. *Inorg. Chem.* **2012**, *51*, 1233.

(7) (a) Sessoli, R.; Powell, A. K. *Coord. Chem. Rev.* **2009**, *253*, 2328. (b) Lin, P. H.; Burchell, T. J.; Clérac, R.; Murugesu, M. *Angew. Chem., Int. Ed.* **2008**, *47*, 8848.

(8) For examples, see: (a) Zhao, J. P.; Hu, B. W.; Zhang, X. F.; Yang, Q.; Fallah, M. S. E.; Ribas, J.; Bu, X. H. *Inorg. Chem.* **2010**, *49*, 11325. (b) Bao, X.; Leng, J. D.; Meng, Z. S.; Lin, Z. J.; Tong, M. L.; Nihei, M.; Oshio, H. *Chem.—Eur. J.* **2010**, *16*, 6169.

(9) Holm, R. H.; Kennepohl, P.; Solomon, E. I. *Chem. Rev.* **1996**, *96*, 2239.

(10) (a) Wang, Y. Q.; Zhang, X. M.; Li, X. B.; Wang, B. W.; Gao, E. Q. *Inorg. Chem.* **2011**, *50*, 6314. (b) Luo, F.; Liao, Z. W.; Song, Y. M.; Huang, H. X.; Tian, X. Z.; Sun, G. M.; Zhu, Y.; Yuan, Z. Z.; Luo, M. B.; Liu, S. J.; Xu, W. Y.; Feng, X. F. *Dalton Trans.* **2011**, *40*, 12651. (c) Bogani, L.; Sangregorio, C.; Sessoli, R.; Gatteschi, D. *Angew. Chem., Int. Ed.* **2005**, *44*, 5817.

(11) (a) Li, D. P.; Wang, T. W.; Li, C. H.; Liu, D. S.; Li, Y. Z.; You, X. Z. *Chem. Commun.* **2010**, *46*, 2929. (b) Boudreaux, E. A.; Mulay, L. N. *Theory and applications of molecular paramagnetism*; Wiley: New York, 1976.

(12) (a) Abbas, G.; Lan, Y.; Kostakis, G. E.; Wernsdorfer, W.; Anson, C. E.; Powell, A. K. *Inorg. Chem.* **2010**, *49*, 8067. (b) Raebiger, J. W.; Miller, J. S. *Inorg. Chem.* **2002**, *41*, 3308.

(13) (a) Rinck, J.; Novitchi, G.; Heuvel, W. V. D.; Ungur, L.; Lan, Y. H.; Wernsdorfer, W.; Anson, C. E.; Chibotaru, L. F.; Powell, A. K. *Angew. Chem., Int. Ed.* **2010**, *49*, 7583. (b) Zheng, Y. Z.; Evangelisti, M.; Winpenny, R. E. P. *Angew. Chem., Int. Ed.* **2011**, *50*, 3692. (c) Mereacre, V.; Prodius, D.; Lan, Y. H.; Turta, C.; Anson, C. E.; Powell, A. K. *Chem.—Eur. J.* **2011**, *17*, 123.

(14) For examples, see: (a) Li, Z. X.; Zeng, Y. F.; Ma, H.; Bu, X. H. *Chem. Commun.* **2010**, *46*, 8540. (b) Hu, B. W.; Zhao, J. P.; Yang, Q.; Zhang, X. F.; Evangelisti, M.; Sañudo, E. C.; Bu, X. H. *Dalton Trans.* **2010**, *39*, 11210. (c) Zhao, J. P.; Yang, Q.; Liu, Z. Y.; Zhao, R.; Hu, B. W.; Du, M.; Bu, X. H. *Chem. Commun.* **2012**, *48*, 6568. (d) Zeng, Y. F.;

Xu, G. C.; Hu, X.; Chen, Z.; Bu, X. H.; Gao, S.; Sañudo, E. C. *Inorg. Chem.* **2010**, *49*, 9734.
(15) Madison, W. I. *SAINT Software Reference Manual*; Bruker AXS: Madison, WI, 1998.
(16) Sheldrick, G. M. *SHELXTL NT Version 5.1. Program for Solution and Refinement of Crystal Structures*; University of Göttingen: Göttingen, Germany, 1997.
(17) For examples, see: (a) Yuan, N.; Sheng, T. L.; Tian, C. B.; Hu, S. M.; Fu, R. B.; Zhu, Q. L.; Tan, C. H.; Wu, X. T. *CrystEngComm* **2011**, *13*, 4244. (b) Sun, Y. Q.; Zhang, J.; Chen, Y. M.; Yang, G. Y. *Angew. Chem., Int. Ed.* **2005**, *44*, 5814. (c) Liu, M. S.; Yu, Q. Y.; Cai, Y. P.; Su, C. Y.; Lin, X. M.; Zhou, X. X.; Cai, J. W. *Cryst. Growth Des.* **2008**, *8*, 4083.
(18) (a) Huang, Y. G.; Wang, X. T.; Jiang, F. L.; Gao, S.; Wu, M. Y.; Gao, Q.; Wei, W.; Hong, M. C. *Chem.—Eur. J.* **2008**, *14*, 10340. (b) Zou, L. F.; Zhao, L.; Guo, Y. N.; Yu, G. M.; Guo, Y.; Tang, J. K.; Li, Y. H. *Chem. Commun.* **2011**, *47*, 8659. (c) Sun, M. L.; Zhang, J.; Lin, Q. P.; Yin, P. X.; Yao, Y. G. *Inorg. Chem.* **2010**, *49*, 9257.
(19) (a) Sharples, J. W.; Zheng, Y. Z.; Tuna, F.; McInnes, E. J. L.; Collison, D. *Chem. Commun.* **2011**, *47*, 7650. (b) Lin, S. Y.; Zhao, L.; Ke, H. S.; Guo, Y. N.; Tang, J. K.; Guo, Y.; Dou, J. M. *Dalton Trans.* **2012**, *41*, 3248. (c) Luzon, J.; Bernot, K.; Hewitt, I. J.; Anson, C. E.; Powell, A. K.; Sessoli, R. *Phys. Rev. Lett.* **2008**, *100*, 247205. (d) Ke, H. S.; Gamez, P.; Zhao, L.; Xu, G. F.; Xue, S. F.; Tang, J. K. *Inorg. Chem.* **2010**, *49*, 7549.
(20) (a) Li, M. Y.; Lan, Y. H.; Ako, A. M.; Wernsdorfer, W.; Anson, C. E.; Buth, G.; Powell, A. K.; Wang, Z. M.; Gao, S. *Inorg. Chem.* **2010**, *49*, 11587. (b) Liu, S. J.; Xue, L.; Hu, T. L.; Bu, X. H. *Dalton Trans.* **2012**, *41*, 6813. (c) Dreiser, J.; Pedersen, K. S.; Piamonteze, C.; Rusponi, S.; Salman, Z.; Ali, Md. E.; Schau-Magnussen, M.; Thuesen, C. A.; Piligkos, S.; Weihe, H.; Mutka, H.; Waldmann, O.; Oppeneer, P.; Bendix, J.; Nolting, F.; Brune, H. *Chem. Sci.* **2012**, *3*, 1024.
(21) (a) Guo, Y. N.; Xu, G. F.; Wernsdorfer, W.; Ungur, L.; Guo, Y.; Tang, J. K.; Zhang, H. J.; Chibotaru, L. F.; Powell, A. K. *J. Am. Chem. Soc.* **2011**, *133*, 11948. (b) Joarder, B.; Chaudhari, A. K.; Rogez, G.; Ghosh, S. K. *Dalton Trans.* **2012**, *41*, 7695. (c) Guo, F. S.; Liu, J. L.; Leng, J. D.; Meng, Z. S.; Lin, Z. J.; Tong, M. L.; Gao, S.; Ungur, L.; Chibotaru, L. F. *Chem.—Eur. J.* **2011**, *17*, 2458.
(22) Habib, F.; Long, J.; Lin, P. H.; Korobkov, I.; Ungur, L.; Wernsdorfer, W.; Chibotaru, L. F.; Murugesu, M. *Chem. Sci.* **2012**, *3*, 2158.
(23) Liu, C. S.; Du, M.; Sañudo, E. C.; Echeverria, J.; Hu, M.; Zhang, Q.; Zhou, L. M.; Fang, S. M. *Dalton Trans.* **2011**, *40*, 9366.
(24) Miao, Y. L.; Liu, J. L.; Li, J. Y.; Leng, J. D.; Ou, Y. C.; Tong, M. L. *Dalton Trans.* **2011**, *40*, 10229.
(25) Bartolomé, J.; Filoti, G.; Kuncser, V.; Schinteie, G.; Mereacre, V.; Anson, C. E.; Powell, A. K.; Prodius, D.; Turta, C. *Phys. Rev. B* **2009**, *80*, 014430.
(26) (a) Lin, P.; Burchell, T. J.; Ungur, L.; Chibotaru, L. F.; Wernsdorfer, W.; Murugesu, M. *Angew. Chem., Int. Ed.* **2009**, *48*, 9489. (b) Guo, Y. N.; Xu, G. F.; Gamez, P.; Zhao, L.; Lin, S. Y.; Deng, R. P.; Tang, J. K.; Zhang, H. J. *J. Am. Chem. Soc.* **2010**, *132*, 8538.
(27) Hewitt, I. J.; Lan, Y.; Anson, C. E.; Luzon, J.; Sessoli, R.; Powell, A. K. *Chem. Commun.* **2009**, 6765.